Dynamics of three-dimensional vesicles in dc electric fields

Ebrahim M. Kolahdouz and David Salac

Phys. Rev. E **92**, 012302 — Published 2 July 2015

DOI: 10.1103/PhysRevE.92.012302

Dynamics of Three-Dimensional Vesicles in DC Electric Fields

Ebrahim M. Kolahdouz and David Salac*
318 Jarvis Hall, Buffalo, NY 14226

A numerical and systematic parameter study of three-dimensional vesicle electrohydrodynamics is presented to investigate the effects of varying electric field strength and different fluid and membrane properties. The dynamics of vesicles in the presence of DC electric fields is considered, both in the presence and absence of linear shear flow. For suspended vesicles it is shown that the conductivity ratio and viscosity ratio between the interior and exterior fluids, as well as the vesicle membrane capacitance, substantially affect the minimum electric field strength required to induce a full Prolate-Oblate-Prolate transition. In addition, there exists a critical electric field strength above which a vesicle will no longer tumble when exposed to linear shear flow.

I. INTRODUCTION

The interaction of lipid vesicles with external electric fields has been a subject of growing interest from both an application and a mechanistic standpoint [1–3]. Recent experimental investigations have demonstrated a number of transient dynamics when vesicles are exposed to electric fields. Cylindrical shapes, with high curvature regions, have been observed in both AC and DC fields [3–5]. If the applied electric potential is not carefully controlled electroporation and destruction of the vesicle is possible [6–8]. As vesicles form a model system for more complicated biological cells, such as red blood cells [9], valuable information about both systems can be obtained by investigating the behavior of vesicles in electric fields.

One of the most interesting behaviors in vesicle electrohydrodynamics is the Prolate-Oblate-Prolate (POP) transition [10–12]. Consider a prolate vesicle where the major axis is initially aligned with the applied electric field, Fig. 1(a). The fluid encapsulated by the vesicle has a different electrical conductivity than the surrounding fluid. The lipid bilayer membrane is impermeable to ions and therefore charges accumulate on both sides of the membrane. As the electrical conductivities differ between the inner and outer fluid the rate at which charges are supplied to the interface is not matched. This gives the membrane a capacitive feature which is responsible for the dynamics of the vesicle in the presence of electric fields.

During this charge accumulation process variations in the Maxwell stress result in membrane forces which act on the surrounding fluid. Under certain conditions this will cause the vesicle to deform from the initial prolate shape to an oblate one, where the major axes are now perpendicular to the electric field, see Fig. 1(b). Over time the vesicle interior becomes electrically shielded from the external electric field and the forces on the membrane result in the vesicle evolving back into the prolate shape (aligned with the electric field), which is always the final membrane shape [10, 12]. In order to observe the full POP transition the external electric field has to be strong enough to overcome other forces present in the membrane and the surrounding fluid. This behavior is of particular interest as a benchmark problem to evaluate numerical algorithms in the modeling of vesicle electrohydrodynamics.

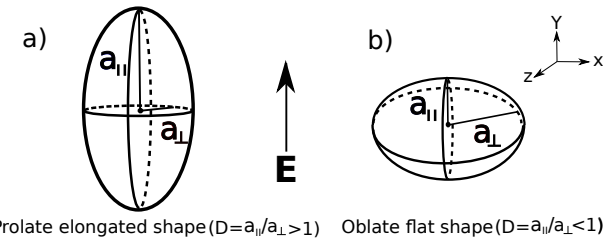

FIG. 1. Sketch of the prolate and oblate shapes and their orientations with respect to the external electric field. The deformation parameter D is defined as the ratio of the axis length in the direction parallel to the field $a_{\parallel}$ to the axis length perpendicular to the field $a_{\perp}$.

Of additional interest is the interaction of a vesicle, a DC electric field, and an externally applied fluid flow. Many cells in the body, such as red blood cells, and biotechnological application of lipid vesicles, such as their use as drug delivery mechanisms, are suspended in non-stationary fluids. It has been previously demonstrated that vesicles exposed to shear flow undergo three basic types of behavior: tank-treading, tumbling, and breathing/trembling, with the viscosity ratio between the inner and outer fluid playing a crucial role in determining the behavior [13–15]. In the tank-treading regime a vesicle aligns at an equilibrium inclination angle with respect to the shear flow. As the viscosity ratio is increased the vesicle begins to tumble end-over-end in a rigid like manner. In an intermediate dynamic, called breathing or trembling, vesicles have large periodic deformations while also undergoing a tumbling like dynamic. Recent theoretical work has demonstrated that the application of a DC electric field can be used to disrupt this behavior [16]. Knowledge about the influence of controllable fields on the dynamics of vesicles in externally driven fluid flows is crucial to advance vesicle-based technologies.

Over the past decade a number of experimental works investigating vesicles exposed to electric fields have begun to appear [1–3, 6, 12]. In physical experiments capturing a full POP transition with a single DC pulse is

* Corresponding author: davidsal@buffalo.edu

not a trivial task [12, 17]. Therefore, attention has also been directed towards theoretical and numerical methods that can provide insight into the electrohydrodynamics of vesicles without many of the difficulties associated with experiments. In an early theoretical work the evolution of a spherical vesicle into a prolate ellipsoid in the presence of AC and DC fields was investigated[18]. A related work determined the membrane bending rigidity from the vesicle deformation [19]. In another work oblate and prolate deformations were predicted in the presence of an applied AC electric field [20]. In more recent analytical studies fluid effects have been taken into account. However, most of these models are limited to nearly spherical vesicles [9, 10] or planar membranes [21, 22] and make the Stokes assumption for the fluid flow. In another two works large ellipsoidal deformations were considered but application of the model to address large shape deformations such as POP were not addressed [8, 23].

In this paper a recently developed model of vesicle electrohydrodynamics is used to carry out a systematic parameter study of a three-dimensional vesicle in the presence of DC electric fields and fluid flow. A full Navier-Stokes solver is employed which is able to capture possible inertia effects in the vesicle dynamics arising from the higher Reynolds number of electrohydrodynamic problems. The effects of fluid and vesicles properties on the electrohydrodynamic behavior are examined and the critical electric field strength required to observe a full POP transition is determined. This includes the effect of membrane capacitance and of the viscosity and conductivity ratios of the embedded and surrounding fluids for a range of vesicle sizes. Vesicles in the presence of combined shear flow and DC electric fields are also investigated and the critical field strength required to transition a vesicle from the tumbling to the tank-treading regime is determined for two vesicle sizes and various viscosity ratios.

II. THE MATHEMATICAL MODEL AND NUMERICAL METHODS

The model used in this paper employs the computational approach presented by the authors in Ref. [16]. Consider a three-dimensional vesicle suspended in an aqueous solution. Deviation from sphericity of the vesicle shape is measured by a reduced volume parameter, v, defined as the ratio of the vesicle volume, V, to the volume of a sphere with the same surface area, A. Therefore the reduced volume can be written as $v = 3V/(4\pi r_0^3)$ where $r_0 = \sqrt{A/4\pi}$ is chosen as the characteristic length scale for the given vesicle. The inner and outer fluids may have differing fluid viscosity and conductivity. The membrane is assumed to be inextensible with constant enclosed volume and surface area. Using the Helfrich model [24] the sum of the membrane forces in three dimensions can be written as

$$\boldsymbol{t}_{mem} = -\kappa_c(\frac{H^3}{2} - 2HK + \nabla_s^2 H)\boldsymbol{n} + \gamma H\boldsymbol{n} - \nabla_s\gamma, \quad (1)$$

where $\boldsymbol{n}$ is the outward facing normal vector on the interface (into the exterior fluid), γ is the interface tension, κ_c is the bending rigidity, H is the total curvature (sum of principle curvatures) and K is the Gaussian curvature at the interface. The quantity $\nabla_s = \left(\boldsymbol{I} - \boldsymbol{n}\boldsymbol{n}^T\right)\nabla$ is the surface gradient operator.

For a vesicle in the presence of an external electric field these forces are balanced by the sum of the hydrodynamic and electric stresses. The hydrodynamic stress at the interface is given as

$$\boldsymbol{\tau}_{hd} = \boldsymbol{n}\cdot[\boldsymbol{T}_{hd}] = \boldsymbol{n}\cdot\left(\boldsymbol{T}_{hd}^{+} - \boldsymbol{T}_{hd}^{-}\right), \quad (2)$$

where $\boldsymbol{T}_{hd} = -p\boldsymbol{I} + \mu(\nabla\boldsymbol{u} + \nabla^T\boldsymbol{u})$ is the bulk hydrodynamic stress tensor while μ, $\boldsymbol{u}$ and p refer to viscosity, fluid velocity, and pressure, respectively. The + sign is used when the interface is approached from the outer fluid while the − sign represents the interface being approached from the inner fluid. Square brackets, [ ], indicate the jump of a quantity across the interface.

The electric field stress at the interface is expressed as

$$\boldsymbol{\tau}_{el} = \boldsymbol{n}\cdot[\boldsymbol{T}_{el}] = \boldsymbol{n}\cdot\left(\boldsymbol{T}_{el}^{+} - \boldsymbol{T}_{el}^{-}\right), \quad (3)$$

with the Maxwell tensor, $\boldsymbol{T}_{el}$, given as $\boldsymbol{T}_{el} = \epsilon(\boldsymbol{E}\otimes\boldsymbol{E} - \frac{1}{2}(\boldsymbol{E}\cdot\boldsymbol{E})\boldsymbol{I})$, where $\boldsymbol{E} = -\nabla\Phi$ is the electric field, ϵ the permittivity, and Φ is the electric potential field.

By employing a level set method to implicitly track the interface varying fluid properties at any point in the domain can be written in a single relation, *e.g.* $\mu(\boldsymbol{x}) = \mu^- + (\mu^+ - \mu^-)\mathcal{H}(\phi(\boldsymbol{x}))$ where $\mathcal{H}$ is the Heaviside function and ϕ is the level set function. One is therefore able to write the momentum equations of binary fluids with varying properties into one single formulation.

Define the viscosity ratio as $\eta = \mu^-/\mu^+$ and introduce t_0, u_0, and E_0 as the characteristic time, velocity, and electric field. Note that the characteristic velocity relates to the characteristic time and length by $u_0 = r_0/t_0$. Three important dimensionless quantities can be defined as $Ca = \mu^+(1+\eta)r_0^3/(t_0\kappa_c)$, $Mn = t_0\epsilon^+E_0^2/(\mu^+(1+\eta))$ and $Re = \rho u_0^2 t_0/\mu^+$. The quantity Ca indicates the strength of the bending forces while Mn indicates the strength of the electric field effects, both with respect to viscous effect, and Re is the Reynolds number. This allows for the single-fluid formulation of the Navier-Stokes equation to be written as [16]

$$\begin{aligned}\rho\frac{D\boldsymbol{u}}{Dt} =& -\nabla p + \frac{1}{Re}\nabla\cdot\left(\mu\left(\nabla\boldsymbol{u} + \nabla^T\boldsymbol{u}\right)\right)\\ &+ \delta(\phi)\|\nabla\phi\|\left(\nabla_s\gamma - \gamma H\nabla\phi\right)\\ &+ \frac{1}{Ca\,Re}\delta(\phi)\left(\frac{H^3}{2} - 2KH + \nabla_s^2 H\right)\nabla\phi\\ &+ \frac{Mn}{Re}\delta(\phi)\|\nabla\phi\|\left[\epsilon\left(\boldsymbol{E}\otimes\boldsymbol{E} - \frac{1}{2}(\boldsymbol{E}\cdot\boldsymbol{E})\boldsymbol{I}\right)\right]\cdot\boldsymbol{n},\end{aligned} \quad (4)$$

where $\delta(\phi)$ is the Dirac delta function and all fluid properties are normalized with respect to the external fluid values. In addition to the momentum balance equations, the fluid incompressibility and surface inextensibility constraints are given as $\nabla\cdot\boldsymbol{u} = 0$ and $\nabla_s\cdot\boldsymbol{u} = 0$,

respectively. Note that in Eq. (4) all quantities are nondimensionalized and the singular contributions of the bending, tension, and electric field forces have been transformed into localized body force terms using the level set and Dirac delta functions.

The leaky-dielectric model is used to obtain the electric potential in the domain. The electric potential is the solution to the Laplace equation in each region, $\nabla^2\Phi^{\pm} = 0$, with an electric potential jump at the interface due to the capacitive property of the membrane. This potential jump is called trans-membrane potential, V_m, and evolves over time by the non-dimensional relation,

$$\bar{C}_m \frac{\partial V_m}{\partial t} + \boldsymbol{u} \cdot \nabla \left(\bar{C}_m V_m \right) = \boldsymbol{n} \cdot \boldsymbol{E}^{+}, \tag{5}$$

where $\bar{C}_m = (C_m r_0)/(t_0 s^+)$ is the non-dimensional membrane capacitance, C_m is the actual capacitance of the membrane, and $s^{\pm}$ is the fluid electrical conductivity of the inner and outer fluid. Note that any trans-membrane conductance is currently ignored. In this work an immersed interface method is used to take into account the time-varying trans-membrane potential and the discontinuous fluid conductivities. This is done by deriving jump conditions for the electric potential and its first and second derivatives in order to achieve second order accuracy. For details of the numerical implementation interested readers are referred to Ref. [25].

For the electrohydrodynamic computations with no imposed shear flow the characteristic time, t_0, is set to the membrane charging time scale, *i.e.* $t_0 = t_m$. For a spherical vesicle this time is given as $t_m = (r_0 C_m / s^+)\,(1/\lambda + 1/2)$, where $\lambda = s^-/s^+$ is the conductivity ratio between the two fluids [7, 26]. Typical experimental values reported for physical properties are given as $r_0 \approx 20$ μm, $\kappa_c \approx 10^{-19}$ J, $s^+ \approx 10^{-3}$ S/m, $\epsilon^+ = \epsilon^- \approx 10^{-9}$ F/m, $C_m \approx 10^{-2}$ F/m^2, $\rho \approx 10^3$ kg/m^3, $\mu^- = \mu^+ \approx 10^{-3}$ Pa s and an electric field strength of $E_0 = 10^5$ V/m [4, 8, 12]. Using these values the dimensionless parameters in the presence of an external electric field and in absence of shearing flow are found to be $Re = 0.19$, $Ca = 3.8 \times 10^4$, $Mn = 18$ and $\bar{C}_m = 0.1$.

If the vesicle under the combined effects of electric field and imposed shear flow is considered the time scale associated with the applied shear flow is chosen as the characteristic time, *i.e.* $t_0 = t_{\dot{\gamma}} = \dot{\gamma}_0^{-1}$ where $\dot{\gamma}_0 \approx 1$ s^{-1} is the applied shear rate. In this situation the corresponding dimensionless parameters are $Re = 10^{-3}$, $Ca = 10$ and $\bar{C}_m = 2 \times 10^{-4}$. Note that when both shear flow and an electric field are applied only weak electric fields are considered and thus the dimensionless strength of the electric field is within the range of $Mn = 10$.

The moving interface is modeled through the use of a semi-implicit, gradient-augmented level set jet scheme which is an extension of the original jet scheme introduced in Ref. [27]. The semi-implicit algorithm is implemented in three steps. The first step is the Lagrangian advection of the cell centers. In the second step the values at the cell centers are smoothed using a semi-implicit scheme. This is done based on introducing a smoothing operator similar to the idea used in Refs. [28, 29]. In the third step the center values are projected back to grid points and the jet of the solution including the gradients are updated; see Ref. [16] for implementation details.

To tackle the hydrodynamic problem a recently developed Navier-Stokes projection method is used. Both local and global fluid incompressibility and surface inextensibility conditions are satisfied in the numerical method by splitting the pressure and tension correction terms into spatially-constant and spatially-varying components and solving for the system of unknowns through the use of a Schur complement decomposition strategy. For details of the numerical approach and the special discretization see Ref. [16].

III. RESULTS

In all the present simulations the vesicle surface area is fixed to 4π and the initial shape is a prolate ellipsoidal vesicle. The computational domain is a box with the size of $[-4.5, 4.5]^3$. Periodic boundary conditions are taken in the $x-$ and $z-$directions while wall-boundary-conditions are taken in the $y-$direction. The electric field is imposed by setting an electric potential equal to $\Phi = -y$ on the wall-boundaries. In the case where shear flow is also applied the velocity at the wall-boundaries is taken to be $u = y$. Note that the electric field and fluid velocity have been normalized by E_0 and u_0. A Cartesian collocated mesh with uniform grid spacing is used and the grid spacing is chosen to be $h = 0.075$ with a time-step of $\Delta t = 5 \times 10^{-4}$. Further information about the domain size, time step, and grid spacing choices can be found in Ref. [16].

First consider the behavior of a vesicle in the absence of an externally applied shear flow. The vesicle configuration is described by the deformation parameter:

$$D = \frac{a_{\parallel}}{a_{\perp}}, \tag{6}$$

where $a_{\parallel}$ is the axis length of the vesicle in the direction parallel to the applied electric field and $a_{\perp}$ is the length of the axes perpendicular to the electric field, see Fig. 1. A prolate shape is given by $D > 1$ (major axis aligned with the direction of the electric field) while the oblate shape has $D < 1$ (major axis perpendicular to the direction of the electric field). The deformation parameter, D, is directly calculated from the interface location as described by the level set.

The electrical properties of the two fluids, including the permittivity and electric conductivity, are among the most important factors in determining the dynamics of vesicles exposed to external DC electric fields. The ratio of the electric permittivity to the electric conductivity in each fluid gives the bulk charge relaxation time expressed as $t_c^{\pm} = \epsilon^{\pm}/s^{\pm}$ [10]. This time represents the rate at which each fluid can supply charges to the interface which is different for fluids with different electrical properties. The ratio of the charge relaxation time of the interior

fluid to the exterior fluid is given by $t_c^-/t_c^+ = \zeta/\lambda$ where $\zeta = \epsilon^-/\epsilon^+$ and $\lambda = s^-/s^+$. This measure is of major importance in vesicle electrohydrodynamics and shows the competition between the two fluids in conducting charges towards the membrane. For typical vesicle experiments it is reasonable to assume $\zeta = 1$ and hence the deviation of the conductivity ratio from one is the factor that determines different vesicle dynamics.

To illustrate the types of deformations in a full POP transition and how it compares to an incomplete transition the shape of a vesicle with two different electric field strengths, represented by Mn, are presented in Fig. 2 for an applied electric field in the vertical direction. The bottom row of results are for a strong electric field with $Mn = 28$ while a weaker field, $Mn = 20$, is used for the results in the top row. In the former case, the electric forces are strong enough to overcome the other membrane forces of the vesicle and the viscous forces of the fluid, which drives the vesicle into the oblate state where $D < 1$. However, when the weak electric field is applied the initially prolate vesicle transitions into a slightly less prolate profile but is unable to obtain the full prolate to oblate transition. Note that the final shape is the same in both cases. This indicates that there exists a critical electric field strength, Mn_c, above which a full POP transition occurs to a suspended vesicle exposed to an external DC field. As will be shown below, this critical electric field strength depends on a number of material parameters including the membrane capacitance, $\bar{C}_m$, and the reduced volume, v, of the vesicle, as well as the conductivity ratio, λ, and the viscosity ratio, η, of the two fluids.

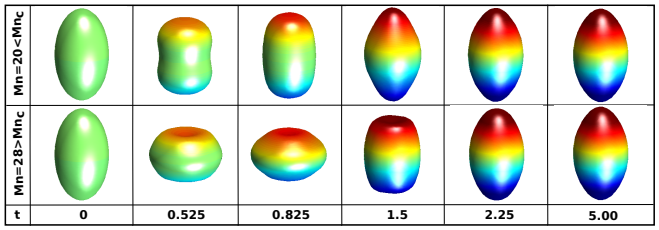

FIG. 2. (Color Online) Simulation results showing the full POP transition (bottom series) vs. a vesicle that remains in the prolate regime (top series) for a vertically applied electric field. The reduced volume in both simulations is $v = 0.93$ and other simulation parameters are set to $Re = 0.19$, $Ca = 3.8 \times 10^4$, $\bar{C}_m = 0.1$, $\lambda = 0.1$ and $\eta = 1.0$. The colors on the surface (online version) indicate the distribution of the trans-membrane potential over time, with darkest blue (lower pole) indicating a membrane potential of $V_m = -1.6$ and darkest red (upper pole) indicating a membrane potential of $V_m = 1.6$.

To study the role of the fluid conductivity ratio in POP dynamics the critical Mason number, Mn_c, is determined for various conductivity ratios. This behavior is illustrated in Fig. 3 for a range of different reduced volumes. The region above each curve shows where the POP transition occurs while the region below the curves indicates the Mn values that are not strong enough to force the vesicle to full POP transition. As the the conductivity ratio λ increases, larger and larger electric field strengths are required to induce the POP transition. Theoretically

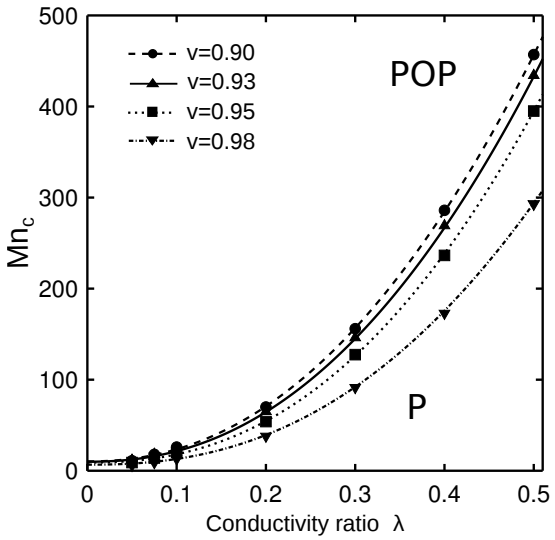

FIG. 3. The effect of the conductivity ratio, λ, on the POP transition. The region above the curve shows where the POP transition occurs while the region below the curve represents a vesicle that remains prolate for all the time. The transition is plotted for four different reduced volumes, $v = 0.90$, 0.93, 0.95, and 0.98. The two regions are separated by the critical field strength, Mn_c, where the dynamics change from purely prolate to prolate-oblate-prolate. The nondimensional parameters are set to $Re = 0.19$, $Ca = 3.8 \times 10^4$, $\eta = 1.0$ and $\bar{C}_m = 0.1$.

speaking, for a vesicle with $\lambda = 1$, *i.e.* matched conductivity between the two fluids, the Mn_c approaches infinity. In fact, as will be demonstrated in Sec. III it is not possible for a vesicle with match conductivity to achieve a POP transition.

The membrane capacitance is another important factor in determining the dynamics of the vesicle in a DC field. In particular, the capacitance appears as a primary parameter in the time scale associated with the membrane charging given, t_m. The larger the capacitance the larger duration of time electric field forces can act on the membrane. In the context of the POP transition an interesting comparison can be made between the membrane charging time scale and the electrohydrodynamic time scale of the applied field given by $t_{ehd} = \mu^+(1+\eta)/(\epsilon^+ E_0^2)$. The electrohydrodynamic time scale largely depends on the electric field strength: a strong electric field is associated with a shorter electrohydrodynamic time. In theory, for a nearly spherical vesicle a full POP transition will occur if $t_{ehd} < t_m$ [12]. In such situations electric field forces have sufficient time to induce a full POP deformation before the trans-membrane potential is saturated at time t_m. As the capacitance increases the charging time of the membrane capacitance, t_m, increases as well which implies that even with a weaker electric field, which results in a larger t_{ehd}, a full POP transition is still possible as long

as t_{ehd} is sufficiently smaller than t_m.

Note that the membrane capacitance affects the amount of deformation as well. An increase of t_m due to larger capacitance leads to larger deformations as the electric forces only influence the dynamics of the membrane in proportion to the time that they are allowed to act. Since the capacitance is a major factor in determining this time the implication is that the deformations are smaller for smaller dimensionless capacitance, $\bar{C}_m$, and deformations grow larger as $\bar{C}_m$ does. This manifests the importance of the membrane capacitance in the type and magnitude of deformations.

Figure 4 shows how changes in the membrane capacitance leads to a vastly different critical field strengths, Mn_c, needed to observe a full POP transition. This behavior is consistent across all investigated vesicle reduced volumes. For the four reduced volumes investigated here the critical field strength scales as the inverse of the membrane capacitance, $Mn_c \propto \bar{C}_m^{-1}$. This relationship will be further discussed in Sec. IV.

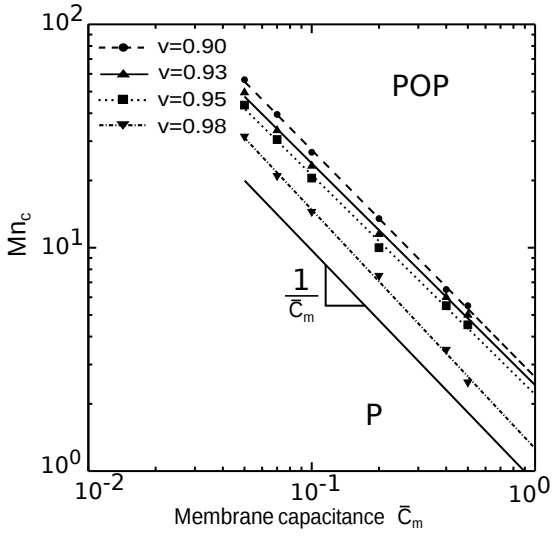

FIG. 4. The effect of the membrane capacitance, $\bar{C}_m$, on the POP transition. The region above the curve shows where the POP transition occurs while the region below the curve represents a vesicle that remains prolate for all the time. The transition is plotted for four different reduced volumes, $v = 0.90$, 0.93, 0.95, and 0.98. The two regions are separated by the critical field strength, Mn_c, where the dynamics change from purely prolate to prolate-oblate-prolate. The nondimensional parameters are set to $Re = 0.19$, $Ca = 3.8 \times 10^4$, $\eta = 1.0$ and $\lambda = 0.1$.

The effect of the viscosity ratio, η, on the dynamics of the vesicle is shown in Fig. 5 for four different reduced volumes. Numerical experiments demonstrate that as η increases a stronger electric field is needed to overcome the resisting hydrodynamic forces of the fluids. A larger viscosity ratio is associated with a larger viscous damping force which in turn leads to slower dynamics and thus a stronger electric field is required to induce the full POP transition. The critical electric field strength appears to be linearly related to the viscosity, $Mn_c \propto \eta$, with the proportionality constant depending on the vesicle size (reduced volume).

One consequence of these results is that it appears that given the same electrical properties, smaller reduced volumes require a stronger field to achieve a full POP transition. This is most likely dependent on the initial shape, as smaller reduced volumes begin as more prolate (more stretched out) vesicles. This means that as the reduced volume decreases larger deformations are required to obtain the prolate-oblate transition. Future work will investigate this, as it is possible to have many different initial vesicle shape conditions for the same reduced volume.

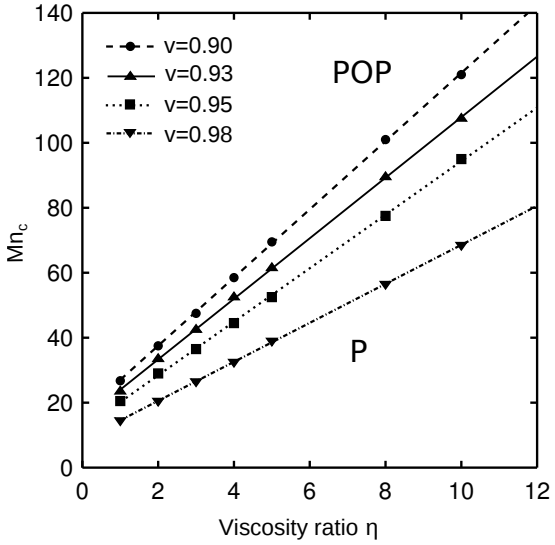

FIG. 5. The viscosity ratio effect on the vesicle behavior transition from the prolate regime (region below the curve) to POP regime (region above the curve). The two regions are separated by the critical field strength, Mn_c where the dynamics changes from one to another. This transition is plotted for four different reduced volumes, $v = 0.90$, 0.93, 0.95, and 0.98. The non-dimensional parameters are set to $Re = 0.19$, $Ca = 3.8 \times 10^4$, $\bar{C}_m = 0.1$ and $\lambda = 0.1$.

Next, the combined effects of an electric field and shear flow are considered. In this case the strength of the external electric field is increased from zero to investigate the changes in the dynamics of the vesicle. Note that here the shear flow time scale is used as the characteristic time scale. With typical experimental values this results in non-dimensional parameters of $Re = 10^{-3}$, $Ca = 10$ and $\bar{C}_m = 2 \times 10^{-4}$. For typical situations the shear flow time scale is approximately $t_{\dot{\gamma}} = 1$ s while the membrane charging time scale is approximately 10^{-3} s [16]. Therefore, in this situation the trans-membrane potential is taken to respond instantly to changes in the membrane configuration and is thus at a pseudo-steady-state.

The effect of the electric field is to align the vesicle vertically with the direction of the field. For a vesicle in the tumbling regime an increase in Mn will result in a slower tumbling period. A close observation of vesicle dynamics under the combination of shear and an external weak electric field reveals that the periodic behavior in this situation is more akin to vacillating-breathing mo-

tion where the vesicle does not follow a rigid-body like rotation but instead the poles retract and additional deformations are induced in the shear plane. If the field is strong enough the electric field forces acting against the shearing forces of the fluid can eventually bring the vesicle into an equilibrium inclination angle.

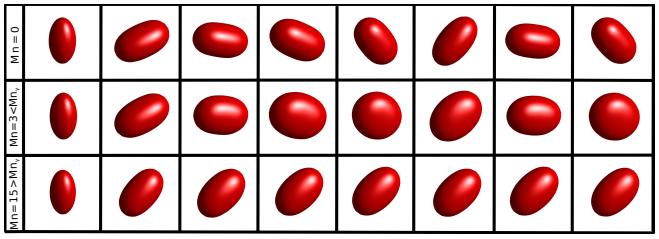

FIG. 6. (Color Online) Dynamics of a vesicle under the combined effects of shearing flow and an applied electric field at various times. The reduced volume is $v = 0.93$ and a viscosity ratio of $\eta = 10$ is used. Other simulation parameters are $Re = 10^{-3}$, $Ca = 10$ and $\bar{C}_m = 2 \times 10^{-4}$. From left to right the snapshots are given at t=0.0, 2.5, 6.0, 7.0, 8.0, 10.0, 15.0, 17.0. The top row shows the tumbling vesicle in the absence of external electric field, $Mn = 0$. The middle row corresponds to a vesicle with a vacillating-breathing like motion under an electric field strength of $Mn = 3$. The bottom row shows a tank-treading vesicle under an strong electric field strength of $Mn = 15$.

These different dynamic regimes are shown in Fig. 6. In this example the vesicle has a reduced volume of $v = 0.93$ and the viscosity ratio is $\eta = 10$. This ratio is larger than the critical viscosity ratio needed to obtain tumbling in shear flow when in the absence of an electric field. The top row in the figure shows the dynamics over time when the electric field is not present in the simulation, $Mn = 0$. As would be expected the vesicle tumbles with the profile of the vesicle remaining nearly constant and rotating periodically in time. The vacillating-breathing like motion is seen for the results shown in the middle row. In this simulation a weak electric field of $Mn = 3$ is used. Unlike the tumbling motion, in this regime the profile of the vesicle undergoes changes over time as it periodically rotates about the vorticity axis. Finally the bottom row demonstrates the vesicle dynamics of the same vesicle under an electric field with a stronger strength, $Mn = 15$. The vesicle reaches an equilibrium, tank-treading inclination angle and stays in that position permanently.

The critical Mason number at which the transition from tumbling like motion (either tumbling or vacillating-breathing) to tank-treading occurs is denoted as Mn_γ. The required Mn_γ for two different reduced volumes over a range of viscosity ratios is plotted in Fig. 7. As is expected, an increase in the viscosity ratio required a stronger electric field to initiate the tumbling to tank-treading transition.

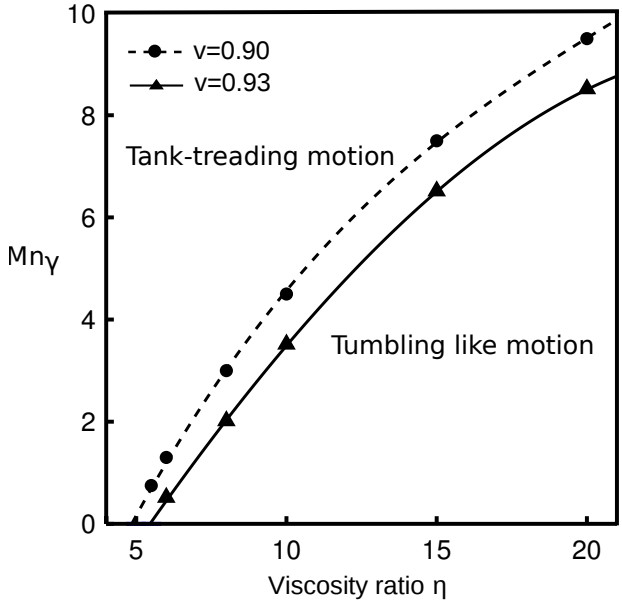

FIG. 7. Tumbling like to tank-treading transition for vesicles with two different reduced volumes, $v = 0.90$ and $v = 0.93$, under the combined effect of imposed shear flow and weak DC electric fields. The non-dimensional parameters are set to $Re = 10^{-3}$, $Ca = 10$, $\chi = 1$, $\bar{C}_m = 2 \times 10^{-4}$ and $\lambda = 0.1$. Membranes with $Mn \neq 0$ have a pseudo-steady-state trans-membrane potential. The region above the curve is the tank-treading regime while the region below the curve shows the tumbling like regime. Increasing the field strength from zero gives rise to a force which counter-acts the motion of a normally tumbling vesicle.

IV. DISCUSSION

To better understand why a vesicle will undergo a prolate-oblate-prolate transition in the presence of an electric field let us consider the electric field forces acting on the membrane. For simplicity and to match the computational results assume that the electric permittivity ratio is one, $\epsilon^+ = \epsilon^-$. Next, consider only the normal electric field forces on the interface. Tangential electric field forces will drag the fluid into motion but do not induced changes in the vesicle membrane.

It is straightforward to write the normal electric force in terms of the normal and tangential components of the electric field,

$$\boldsymbol{\tau}_{el} \cdot \boldsymbol{n} = \frac{\epsilon^+}{2}\left((E_n^{+2} - E_n^{-2}) - (E_t^{+2} + E_b^{+2} - E_t^{-2} - E_b^{-2})\right), \tag{7}$$

where E_t and E_b are the tangential and E_n is the normal electric field at that point. Note that the notation here is $E_n^{+2} = (E_n^+)^2$ and $E_n^{-2} = (E_n^-)^2$.

This clearly shows both normal and tangential electric field components contribution to membrane deformation. To further simplify the discussion, consider the two points A and B located at the top pole and the equator of the vesicle, respectively, see Fig. 8. Due to the axial symmetry there are no tangential components of the

electric field at point A and thus the normal electric field force at that point is simplified to

$$\boldsymbol{\tau}_{el}^{A}\cdot\boldsymbol{n}=\frac{\epsilon^{+}}{2}\left(E_{n}^{+2}-E_{n}^{-2}\right), \tag{8}$$

It should be noted that in the simulations presented in this paper no symmetry is imposed other than the initial condition.

One of the conditions on the interface is the continuity of the Ohmic current $\boldsymbol{J}=s\boldsymbol{E}$ in the normal direction, $(\boldsymbol{J}^{+}-\boldsymbol{J}^{-})\cdot\boldsymbol{n}=s^{+}E_{n}^{+}-s^{-}E_{n}^{-}=0$. It is therefore possible to write $E_{n}^{+}=\lambda E_{n}^{-}$ and thus at point A the normal electric force becomes

$$\boldsymbol{\tau}_{el}^{A}\cdot\boldsymbol{n}=\frac{\epsilon^{+}(\lambda-1)}{2}E_{n}^{-2}. \tag{9}$$

At the equator (point B) the direction of the electric field aligns with the y-direction, and thus there is no normal electric field component. Therefore the force at point B is written as

$$\boldsymbol{\tau}_{el}^{B}\cdot\boldsymbol{n}=\frac{-\epsilon^{+}}{2}\left(E_{t}^{+2}+E_{b}^{+2}-E_{t}^{-2}-E_{b}^{-2}\right). \tag{10}$$

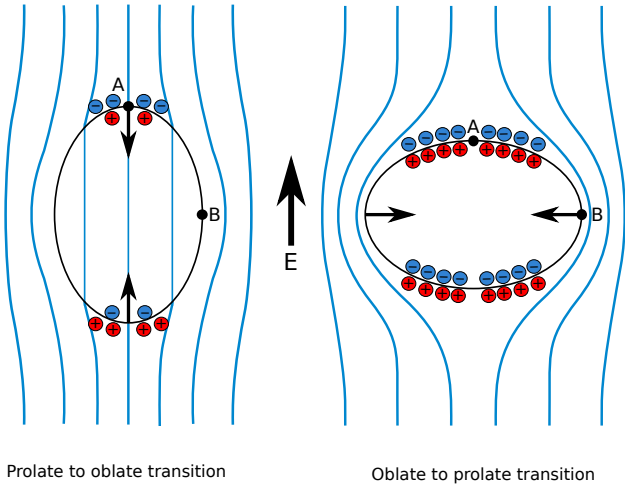

FIG. 8. (Color Online) A sketch of the electric field, induced charges and the dominant electric forces when an initially prolate vesicle is transitioning to the oblate shape (left figure) and when the oblate vesicle is evolving back to the equilibrium prolate transition (right figure).

After the electric field is applied charges from both the enclosed and surrounding fluids start migrating towards the interface. However, due to the differing electric conductivities the charges accumulate at differing rates. This leads to an apparent charge,

$$Q=\epsilon^{+}(E_{n}^{+}-E_{n}^{-}), \tag{11}$$

assuming matching permittivity.

Let the electric potential be activated at time 0. The electric fields inside and outside the vesicle are initially matched and non-zero: $E_{n}^{+}=E_{n}^{-}\neq 0$, $E_{t}^{+}=E_{t}^{-}\neq 0$, and $E_{b}^{+}=E_{b}^{-}\neq 0$. According to Eq. (10) the force along the equator is zero. The direction of the force at the vesicle poles depends on the conductivity ratio. When $\lambda<1$ the normal force is in the $-\boldsymbol{n}$ direction, which is a vertically compressive force. On the other hand, when $\lambda>1$ the force is extensional and thus the POP transition can not occur. This demonstrates the necessary condition of $\lambda<1$ when the fluid permittivities are matched.

Now consider what occurs when $t\to\infty$. Given enough time charges are able to accumulate on both sides of the interface. Therefore eventually $Q=0$ and the electric field inside the vesicle becomes zero, $\boldsymbol{E}^{-}=\boldsymbol{0}$ [12]. Accordingly, for matched permittivity $E_{n}^{-}=E_{n}^{+}=0$ while $E_{t}^{-}=0$ and $E_{b}^{-}=0$. Note that in this case $E_{t}^{+}\neq 0$ and $E_{b}^{+}\neq 0$. From Eq. (8) this results in a zero normal force at point A while along the equator, point B, the normal force reduces to a purely compressive force. Notice that this behavior is independent of the fluid electrical conductivities, indicating that the final shape will always be a prolate one.

Now, a rational behind the influence of the three main parameters investigated here, membrane capacitance, fluid conductivity ratio, and fluid viscosity ratio, on the critical electric field strength needed to obtain a POP transition is presented. First examine the contribution of the membrane capacitance. The membrane capacitance influences how fast the trans-membrane potential reaches a steady state value, Eq. (5). The time it takes for the trans-membrane potential to reach steady state is inversely proportional to $\bar{C}_{m}$. As the amount of time that the electric forces can act on the membrane is directly related to the membrane-charging time, a decrease in t_{m} results in a system which does not have enough time to respond and obtain a full POP transition. Therefore the Mason number must increase at a rate proportional to $\bar{C}_{m}^{-1}$ to ensure that the POP transition occurs.

Next consider the viscosity ratio, η. It was stated in Sec. III that for a POP transition to occur the electrohydrodynamic time, t_{ehd}, needs to be smaller than the membrane charging time, t_{m}. Recall that the electrohydrodynamic time scale increases linearly with an increase in the viscosity ratio, $t_{ehd}\propto 1+\eta$ and that the membrane charging time scale only depends on the particular materials of the membrane, not the applied electric field strength. Therefore, to maintain the relation $t_{ehd}<t_{m}$ the electrohydrodynamic time scale needs to remain constant. This means that the square of the electric field, E_{0}^{2}, must increase linearly to counter-act the increase in $1+\eta$. As $Mn\propto E_{0}^{2}$, it is valid to state that $Mn_{c}\propto 1+\eta$.

The conductivity ratio presents a more complicated picture. Based on the previous discussion only $\lambda<1$ will result in a POP transition and thus all cases with $\lambda\geq 1$ are ignored. Examining t_{m} it is clear that an increase in the conductivity ratio will result in a decrease of the membrane-charging time. This is due to the fact that as $\lambda\to 1$ the fluids are able to supply charges to the interface at the same rate and thus a charge mismatch does not occur. Following the discussion regarding the viscosity ratio, a corresponding decrease in t_{ehd} would be

required for a POP transition to occur. This is achieved by increasing the electric field strength and therefore increasing Mn. Analysis of the equations results in a scaling of $Mn_c \propto (2\lambda)/(2+\lambda)$, which can not account for the rapid increase of Mn_c as λ approaches 1, Fig. 3. It is thus necessary to turn to the forces acting on the membrane and how they relate to λ, Eq. (9). Clearly, as the conductivity ratio approaches 1 the forces acting on the membrane asymptotically approach zero. It is therefore expected that rapid growth of the electric field would be needed to obtain a full POP transition. It is suspected that at small conductivity ratios the increase in Mn_c is dominated by $(2\lambda)/(2+\lambda)$ while as $\lambda \to 1$ the growth seems to be dominated by $(1-\lambda)^{-1}$. While numerical verification of this exponent is not presented here a justification can be obtained by examining Eq. (9) and the definition of the normalized electric field strength, Mn. At $t = 0$ both the force and Mn scale as E_0^2, meaning that an increase in the required force at point A corresponds to a similar increase in Mn. The required force needed to obtain a POP transition should not depend on the fluid conductivity ratio, but instead should depend on quantities such as the vesicle shape and the fluid viscosity ratio. Thus, to maintain the force needed to obtain POP the quantity $(\lambda-1)E_0^2 \propto (\lambda-1)Mn_c$ should remain constant. It follows that $Mn_c \propto (1-\lambda)^{-1}$, where the sign has been changed to have a positive value of Mn_c.

Finally, consider the case of both shear flow and an applied electric field. It has been previously observed that as the reduced volume of a vesicle decreases the viscosity ratio required to obtain a tank-treading to tumbling transition also decreases [15, 30]. Another way to interpret this is that for a given viscosity ratio a vesicle with a small reduced volume is "further" in the tumbling regime than a vesicle with a large reduced volume. Similarly, for a given reduced volume a vesicle with a higher viscosity ratio is also "further" in the tumbling regime than a low viscosity ratio vesicle.

As demonstrated above a fully-charged vesicle always wants to align with the direction of an applied electric field. When the electric field is applied in the direction perpendicular to the shear flow direction this alignment counters the shear forces which account for the tumbling motion. Based on the previous discussion it is expected that the further a vesicle is from the tank-treading/tumbling transition, the higher the electric field alignment force needs to be. This type of behavior is indeed observed, with an increase in the electric field strength needed to obtain a tumbling/tank-treading transition when either the viscosity ratio increases or the reduced volume decreases. Unfortunately, due to the large deformations and lack of symmetry when a vesicle undergoes tumbling it is not possible to formulate a simple scaling relationship as was done for the POP transition.

V. CONCLUDING REMARKS

In this paper a parameter space study of 3D vesicles exposed to DC electric fields was presented. In particular, the focus of this work was on the effects of different fluid and membrane parameters on the transition between prolate and oblate shapes for a suspended vesicle, in addition to the transition from the tumbling to the tank-treading regime of a vesicle under the combined effects of a DC electric field and shear flow.

The electric field strength, indicated by the critical Mason number, Mn_c, required for a POP transition was determined. A decrease in the reduced volume of the vesicle was always accompanied with an increase in the critical Mason number. While an increase in the viscosity ratio between the inner and outer fluids brought about an almost linear increase of Mn_c, the change in the dynamics of the vesicle by varying the conductivity ratio between the two fluids and the membrane capacitance of the vesicle was found to be more dramatic and substantial.

The results of the vesicle behavior under the combined effects of shear flow and weak DC electric fields revealed the remarkable influence of the electric field in changing the standard behaviors of tank-treading and tumbling vesicles. Investigations showed that the application of the electric field generates a force which counter-acts the motion of a tumbling vesicle. If the electric field is strong enough the tumbling vesicle stops the expected end-over-end tumbling behavior and undergoes a tank-treading motion. The critical electric field strength, Mn_γ, for this transition to occur was determined for vesicles with two different reduced volumes over a range of different viscosity ratios.

The results and analysis presented here assumed matched fluid permittivities and only considered a single initial vesicle shape. It is expected that different initial vesicle shapes could result in differing dynamics while the equilibrium shape would remain the same as presented here. Additionally, a relaxation of the matched permittivity condition could result in behavior not observed here. Furthermore, the addition of salt or metallic nanoparticles can dramatically change the dynamics, even for vesicles with conductivity ratios larger than one [4, 31]. Future work will explore how the initial vesicle shape, variations in electrical permittivity, and the inclusion of salts or nanoparticles influence the dynamics of vesicles exposed to DC electric fields.

ACKNOWLEDGMENTS

Authors acknowledge financial support by the U.S. National Science Foundation Grant No. 1253739.

[1] U. Zimmermann and G. A. Neil, *Electromanipulation of cells* (CRC press, 1996).

[2] G. Tresset and S. Takeuchi, Biomedical Microdevices **6**,

213 (2004).
[3] R. Dimova, K. A. Riske, S. Aranda, N. Bezlyepkina, R. L. Knorr, and R. Lipowsky, Soft matter **3**, 817 (2007).
[4] K. A. Riske and R. Dimova, Biophysical journal **91**, 1778 (2006).
[5] A. Said, A. Riske Karin, L. Reinhard, and D. Rumiana, Biophysical Journal **95**, L19 (2008).
[6] K. A. Riske and R. Dimova, Biophysical journal **88**, 1143 (2005).
[7] K. Kinosita Jr, I. Ashikawa, N. Saita, H. Yoshimura, H. Itoh, K. Nagayama, and A. Ikegami, Biophysical journal **53**, 1015 (1988).
[8] M. M. Sadik, J. Li, J. W. Shan, D. I. Shreiber, and H. Lin, Physical Review E **83**, 066316 (2011).
[9] P. M. Vlahovska, R. S. Gracia, S. Aranda-Espinoza, and R. Dimova, Biophysical journal **96**, 4789 (2009).
[10] J. T. Schwalbe, P. M. Vlahovska, and M. J. Miksis, Physical Review E **83**, 046309 (2011).
[11] L. C. McConnell, M. J. Miksis, and P. M. Vlahovska, IMA Journal of Applied Mathematics **78**, 797 (2013).
[12] P. F. Salipante and P. M. Vlahovska, Soft Matter **10**, 3386 (2014).
[13] V. Kantsler and V. Steinberg, Phys. Rev. Lett. **95**, 258101 (2005).
[14] P. M. Vlahovska and R. S. Gracia, Phys. Rev. E **75**, 016313 (2007).
[15] D. Salac and M. J. Miksis, Journal of Fluid Mechanics **711**, 122 (2012).
[16] E. M. Kolahdouz and D. Salac, SIAM Journal on Scientific Computing **Accepted** (2015).
[17] P. Salipante, *Electrohydrodynamics of simple and complex interfaces*, Ph.d dissertation, Brown University (2013).
[18] M. Winterhalter and W. Helfrich, Journal of Colloid and Interface Science **122**, 583 (1988).
[19] M. Kummrow and W. Helfrich, Physical Review A **44**, 8356 (1991).
[20] M.D. Mitov, P. Méléard, M. Winterhalter, M.I. Angelova, and P. Bothorel, Physical Review E **48**, 628 (1993).
[21] J. T. Schwalbe, P. M. Vlahovska, and M. J. Miksis, Physics of Fluids (1994-present) **23**, 041701 (2011).
[22] J. Seiwert, M. J. Miksis, and P. M. Vlahovska, Journal of Fluid Mechanics **706**, 58 (2012).
[23] J. Zhang, J. D. Zahn, W. Tan, and H. Lin, Physics of Fluids (1994-present) **25**, 071903 (2013).
[24] W. Helfrich *et al.*, Z. Naturforsch. c **28**, 693 (1973).
[25] E. M. Kolahdouz and D. Salac, Applied Mathematics Letters **39**, 7 (2015).
[26] T. Y. Tsong, Biophysical Journal **60**, 297 (1991).
[27] B. Seibold, R. R. Rosales, and J.-C. Nave, Discrete and Continuous Dynamical Systems - Series B **17**, 1229 (2012).
[28] E. M. Kolahdouz and D. Salac, SIAM Journal on Scientific Computing **35**, 231 (2013).
[29] P. Smereka, Journal of Scientific Computing **19**, 439 (2003).
[30] V. Kantsler and V. Steinberg, Phys. Rev. Lett. **96**, 036001 (2006).
[31] R. Dimova, N. Bezlyepkina, M. D. Jordo, R. L. Knorr, K. A. Riske, M. Staykova, P. M. Vlahovska, T. Yamamoto, P. Yang, and R. Lipowsky, Soft Matter **5**, 3201 (2009).